Wetting of a fluid interface by a homopolymer: A system with a rich prewetting behavior

F. A. M. Leermakers, C. Dorrepaal, and N. A. M. Besseling

Citation: J. Chem. Phys. **111**, 2797 (1999); doi: 10.1063/1.479557
View online: http://dx.doi.org/10.1063/1.479557
View Table of Contents: http://jcp.aip.org/resource/1/JCPSA6/v111/i6
Published by the American Institute of Physics.

Additional information on J. Chem. Phys.

Journal Homepage: http://jcp.aip.org/
Journal Information: http://jcp.aip.org/about/about_the_journal
Top downloads: http://jcp.aip.org/features/most_downloaded
Information for Authors: http://jcp.aip.org/authors

ADVERTISEMENT

Downloaded 28 Feb 2012 to 137.224.252.10. Redistribution subject to AIP license or copyright; see http://jcp.aip.org/about/rights_and_permissions

Wetting of a fluid interface by a homopolymer: A system with a rich prewetting behavior

F. A. M. Leermakers, C. Dorrepaal, and N. A. M. Besseling
Laboratory of Physical Chemistry and Colloid Science, Wageningen Agricultural University, Dreijenplein 6, 6703 HB Wageningen, The Netherlands

(Received 19 February 1999; accepted 7 May 1999)

A lattice-based self-consistent-field theory is used to reveal the wetting characteristics of a polymeric phase at an interface between two solvent phases. Both solvents are monomeric and the polymer chains are modeled as freely jointed chains of $N=100$ similar segments. From the polymer point of view we limit our investigations to the symmetric case; both solvents are equally poor for the polymer. We show that the polymer wets the interface both in the limit of strongly and weakly segregated liquids, but that at intermediate values of the L/L demixing the polymer phase can be in a lens configuration (partial wetting). The wetting transitions at strong segregation of the two solvents is always first order, the ones at weak segregation can be either first or second order, depending on the polymer/solvent interactions. For a particular value of the polymer–solvent interaction parameter the two wetting transitions as generated by changing the L/L demixing (then both of the first-order type) merge. At this point the two prewetting lines still exist and obviously merge as well. It is further possible to find detached ''prewetting'' lines in the regime where the polymer wets the interface at all relevant (i.e., consistent with the presence of three phase coexistence) values of the L/L demixing. Physically this means that there is a range of interfacial widths for which the formation of a new (polymeric) phase is hindered by a free energy barrier at a certain film thickness, but that there is no wetting transition associated with this barrier. © *1999 American Institute of Physics.* [S0021-9606(99)51329-9]

I. INTRODUCTION

The formation of new phases, i.e., demixing of liquids with limited compatibility, is of interest in many applications. Exactly how the new phase is formed and where it is situated in the system, are the primary interests. The first phenomenon is positioned in the domain of nucleation and will not be discussed in this paper. Intimately connected to the formation of a new phase is the creation of interfaces. The phase boundaries play an important role in the system. There are degrees of freedom available to a given system to play with the extend of its interfaces as a function of, e.g., the temperature. Phenomena related to this are studied in the field of wetting. This is the topic of the present, paper. Wetting theory has matured over the last decade and several excellent reviews have been written.[1,2]

We study a polymer phase to be formed or present at a liquid–liquid interface. This system is idealized in several ways. From the polymer point of view we consider the system to be symmetric; the polymer does not favor either one of the solvents. This leaves essentially two interaction parameters in the system. One parameter determines the (finite) solubility of the polymer in the solvents, the other one determines the miscibility of the two solvents and therefore also the width of the interface between them. Upon concentrating the system with polymer we observe the formation of the polymer phase in between the two liquids. The new phase can sit as a lens at the interface (partial wetting) or can separate the two solvent phases (complete wetting). Wetting transitions (changes from partial to complete wetting) can, e.g., be generated by varying the width of the interface at fixed solubility of the polymer in the solvents. We will show below that it is possible to have prewetting characteristics (wetting theory will be outlined below) in a system which behaves non-classical as a function of this control parameter. In particular we show that the prewetting line(s) can be disconnected from the wetting transition(s) for a particular cut through the parameter space. Detached prewetting lines are not forbidden in the general wetting theory, but we are not aware of detailed analysis of it. Our system is still very simple and the results are expected to be significant for applications in, e.g., polymer blends and microemulsion systems.

The remainder of this paper is as follows. First, we will briefly outline the standard theory of wetting and review the characteristics of a statistical mechanical theory which can handle complex inhomogeneous molecular systems (self-consistent-field theory). In the result section we will demonstrate that the interfacial width is an interesting control variable and focus on the prewetting phenomena. In the discussion some attention will be given to possibilities for experimental verification.

II. INTRODUCTION TO WETTING PHENOMENA

The bulk phase diagram of a multicomponent mixture may exhibit so-called solubility gaps[3] [cf. Figs. 1(b) and 1(c)]. This means that overall compositions within such a solubility gap are unstable; the system forms spontaneously separate phases. At equilibrium (no chemical potential gradients) the phases have compositions given by the saturation values (binodals). The amount of each phase is determined

 © 1999 American Institute of Physics

Downloaded 28 Feb 2012 to 137.224.252.10. Redistribution subject to AIP license or copyright; see http://jcp.aip.org/about/rights_and_permissions

by a mass balance (overall composition). The interface between the two phases is minimized such that there is as little contact of one phase with the other. Over a century ago Van der Waals formulated a molecular theory for the structure of the interface formed by two simple liquid phases at coexistence.[4] It was shown that not too far from the critical point the density profile is a hyperbolic tangent. The width of the interface increases and the surface tension decreases upon approaching the critical point. At the critical point the distinction between the two phases ceases to exist, or inversely, when the opposite route is followed, the system passes from having one phase to two phases. Extensions of the van der Waals theory to more than two components is necessary to use such an approach for wetting studies. Below we will use a theory which deals with multiple interfaces and is a van der Waals-type in several ways.

For a three-component system it is possible that three separate phases exist. Let us for convenience denote these phases as α, β, and γ. In this case it may happen that also three different interfaces, $\alpha\beta$, $\alpha\gamma$, and $\beta\gamma$ are present. Then there is also a three-phase contact point where all three phases meet, $\alpha\beta\gamma$. Such contact region can be characterized by contact angles. The contact angle(s) are a function of the three surface tensions of the three interfaces in the system. The necessary relations were, in principle, already specified by Young[5] and Laplace[6] and can be derived from a minimization of the excess free energy.[2] It is also possible that one of the phases sits in between the other two. Then only two, e.g., $\alpha\beta$ and $\beta\gamma$ are present. This condition follows naturally from the three-interface case if the contact angles approach 0 or 180°.

The passing from the condition that the contact angles are finite (one phase sits as a lens-shaped droplet in between the other two), to one where the contact angles are zero (or 180°; one phase sits as a film in between the other two) is a phase transition; the system passes from having three interfaces to the case that there are just two.[1] In wetting language the aforementioned wetting transition is one from partial wetting to complete wetting. By choosing suitable control variables one can often force a system to change its wetting characteristics. Going from partial to complete wetting occurs at a wetting transition which may be a first or a second order phase transition.

To distinguish between the two, let us again consider a three-component system wherein two phases (one rich in one component, the other rich in a second component) exist and let us study the structure of the interface, or more precisely study the accumulation of molecules of the third kind at this interface. Let us thus take the situation that the third component is not completely soluble in the two phases. Then upon the approach of the solubility limit of the third component in this two-phase system the third component will accumulate substantially at the interface. This accumulation (adsorption) is experimentally (and theoretically) accessible (for a graphical example see Fig. 9 below). So-called adsorption isotherms give the adsorbed amount at an interface as a function of the chemical potential of this component. Upon the approach of the solubility limit the adsorption isotherms may reveal information where and how the third phase will be formed. In the case of partial wetting the adsorbed amount remains finite when the saturation value is reached. In the case of complete wetting the adsorbed amount diverges at the saturation value (coexistence value). The order of the wetting transition can be extracted from the evolution of the adsorption isotherms as a function of a suitable control parameter, e.g., the temperature T.

A wetting transition can most easily be observed by examining the adsorbed amount at the coexistence condition (i.e., at the chemical potential defined by the presence of the third macroscopically large phase) as a function of this control variable.[1] As mentioned above, two scenarios exists. (i) One may witness the adsorbed amount to grow continuously upon the increase in temperature and find it to diverge at T^{wet}. This case is not very common and it is called a second-order wetting transition or critical wetting [see Fig. 11(b) below, where the control parameter is not the temperature but an interaction parameter]. (ii) Much more frequently one may find that upon the approach of the wetting temperature the adsorbed amount exhibits a discontinuity; it remains finite for all $T<T^{\mathrm{wet}}$ and it is infinite at $T>T^{\mathrm{wet}}$. This scenario is called a first-order wetting transition. Inspection of the corresponding adsorption isotherms is very instructive. For a range of control variable T (not too far below T^{wet}), at some value of the applied chemical potential (not too far below the coexistence value), the adsorbed amount θ^{exc} exhibits a discontinuity called a prewetting transition; $\lim_{T\downarrow T^{\mathrm{prewet}}}\theta^{\mathrm{exc}}$ is considerably larger than $\lim_{T\uparrow T^{\mathrm{prewet}}}\theta^{\mathrm{exc}}$. In a mean-field theory such a step shows up as a van der Waals loop [see Figs. 2–4 and 11(a) below] from which the ''step'' can be obtained, e.g., by a Maxwell construction. The magnitude of the step grows upon a decrease in temperature and diverges at the wetting temperature T^{wet}. The step shrinks upon an increase in temperature and vanishes at a (prewetting) critical point, T^{pcp}.

In a wetting phase diagram (see, e.g., Fig. 5 below) one can plot the chemical potential at the step in the isotherm against the value the control variable. In this phase diagram these points form a line. This line is called the prewetting line. In the case of a first-order wetting transition it is natural to find a prewetting line in the wetting phase diagram and that this prewetting line is connected to the wetting temperature T^{wet} at the bulk coexistence line, given by $\mu=\mu^{\#}$. In the case of critical wetting such a prewetting line does not exist and the wetting phase diagram only features the bulk coexistence line onto which one point reflects the wetting transition. Below we will show that variation in the wetting phase diagrams may occur even for relatively simple model systems.

One may be interested in forcing a system from a partial wetting condition to complete wetting. Basically just one general guideline exists which is due to Cahn.[7] In a partial wetting condition one will generally have the condition that three phases called α, β, and γ, come together at some point in space characterized by some type of contact angle. Cahn argued that when this system is pushed to the condition that it goes from a three-phase (α,β,γ) to a two-phase $(\alpha\beta,\gamma)$ system at some critical temperature T^{c}, one should expect a wetting transition to occur before the critical temperature is

Downloaded 28 Feb 2012 to 137.224.252.10. Redistribution subject to AIP license or copyright; see http://jcp.aip.org/about/rights_and_permissions

reached. In other words, when the system is sufficiently close to a critical temperature for the α,β mixture, there cannot be a partial wetting condition. We will not repeat the arguments here, but the background is that the interfacial tension of the interface that becomes critical $\sigma(\alpha,\beta)$ scales differently with the relative temperature $(T-T^c)$ than the difference between the (noncritical) interfacial tensions $\sigma(\alpha,\gamma)-\sigma(\beta,\gamma)$. The physical background of the different scaling behavior is that the interface between the liquids that approaches the critical point becomes increasingly diffuse, whereas the noncritical interfaces remain relatively sharp. Therefore both type of interfaces have different entropic and energetic contributions to the interfacial tension and thus respond differently to the change in relative temperature.

Some experimental and theoretical approaches are available in the literature of wetting at liquid–liquid and liquid–air interfaces. Of interest to mention is a recent study of the wetting behavior of alkanes (e.g., pentane, hexane,...) on a water–air interface.[8] This system was found to exhibit nontrivial behavior not predicted by the standard wetting theory. Here an interesting interplay between short- and long-range forces leads to first-order transitions from microscopically to mesoscopically thick layers at coexistence (bulk binodal values), while the system remains in the partial wetting regime. A Cahn-type theory for this case has been proposed.[9] In the present paper we will not consider long-range van der Waals contributions to the wetting problem.

The experimental investigation of the formation of a new phase in a liquid–liquid interface is also feasible. For example, the formation and the wetting characteristics of a microemulsion phase in a Winsor 3 system has been investigated[10,11] and compared to theoretical predictions.[12] We will return to this system below, as it resembles the present system in several ways.

In this paper we will study wetting at an existing liquid–liquid interface in an approach similar in spirit to the one used by Van Eijk and Leermakers.[13] We will use a similar system as these authors. More specifically, we will investigate the case that the existing interface is formed by two monomeric liquids and the new phase is formed by a polymeric one. Van Eijk and Leermakers limited their investigations to the case that the pre-existing interface had a given width (the distance from the critical point of the binary liquid was kept constant) and studied the effects of several parameters such as the degree of polymerization of the polymeric component, and the stiffness of these molecules on the order of the wetting transition. In the present paper we will focus our attention to the effect of the interfacial width and fix other molecular characteristics of the system.

III. THE SCHEUTJENS FLEER SELF-CONSISTENT-FIELD THEORY

To study wetting transitions in complex systems one needs in principle accurate ways to generate adsorption isotherms. This is not a trivial problem as for each point in an adsorption isotherm one has to solve for the equilibrium structure of the inhomogeneous molecular distributions at the interface. Considering that there are nonideal interactions (natural for a system with a solubility gap) and that the molecules may have internal degrees of freedom one needs rather sophisticated models. In passing we note that very few Molecular Dynamics or Monte Carlo simulations exist on these issues.[14] Clearly most wetting theories are on a mean-field level. Classical examples of this are models based on a phenomenological free energy expansion known as the Ginzburg–Landau approach.[1] It is from this branch of mean-field models that the general wetting theory as outlined above has emerged. This method can only be used near the critical points where the interfaces are not sharp. Moreover there is no direct link between the parameters in a Ginzburg–Landau theory and the molecular system that is studied.

A detailed molecular-level theory can be formulated which makes use of self-consistent-field (SCF) approximations.[15,16] We use a lattice-based SCF method first proposed for polymers at interfaces by Scheutjens and Fleer (SF SCF) to model the structure (formation) of a polymer phase at a fluid interface. In the following we will briefly outline the method and concentrate on the problem of wetting at such an interface.

A. The system

Let us consider a system that contains three molecular components, $i,j=P_N,A,B$. Molecule $i=P_N$ is a polymer component composed of N segments of type P, each of size b^3 where b is the length of a segment of the chain. Molecules $i=A$ and $i=B$ are both monomeric $N_A=N_B=1$ and of size b^3 and let the system be within the solubility gap between the two type of molecules. Let us consider the interface between the A-rich and B-rich phases, and let this interface be flat. As told above we are interested in finding the adsorption isotherms of the polymeric component adsorbing at this (macroscopic) interface. Let us assume that the adsorption takes place in a homogeneous way. In this case the symmetry is such that we expect that the main density gradients are perpendicular to the interface and that less important fluctuations in density occur parallel to the interface. This allows us to apply a mean-field approximation parallel to the interface which renders density gradients to be one-dimensional (1D), perpendicular to the interface. This direction will be denoted by z. By applying the local mean-field approximation we ignore that the newly formed polymer-rich phase assumes a lens shape at the interface between the A-rich and B-rich phase. Although a lens would be the stable configuration in the partial wetting regime, this is not necessarily a problem, because from the 1D-adsorption isotherms one will, in such case, notice that part of the isotherm is not stable (as it represents systems that are supersaturated). The macroscopic contact angle of the lens can be found from the evaluation of the interfacial free energies of the thick and thin film at coexistence (stable) conditions. Alternatively, one can set-up a 2D-gradient SCF calculation and calculate the droplet shape of mesoscopically small droplets directly.[17] We will not do this here.

B. The lattice

In the SF SCF theory it is customary to develop the equations in discrete form. Thus a system of discrete coordinates is used which is referred to as a lattice. The character-

Downloaded 28 Feb 2012 to 137.224.252.10. Redistribution subject to AIP license or copyright; see http://jcp.aip.org/about/rights_and_permissions

istic spacing in the lattice is set equal to the monomer size b. Lattice layers parallel to the interface, with L lattice sites each, are formed and the layers are numbered $z=1,...,M$. L is chosen in the macroscopic limit so that edges can be ignored. It is convenient to introduce a priori step probabilities $\lambda_{z-z'}$, where z' takes the three values, $z'=z-1,z,z+1$. For example, a cubic lattice $\lambda_0=4/6$, and $\lambda_1=\lambda_{-1}=1/6$. We note that other types of lattice may be used. The discretisation of the space by means of a lattice is a rather good approximation as long as one is not interested in details that are smaller than the lattice spacing.

C. The SCF formalism

A proper derivation of the SCF equations from an expression for the partition function can be found elsewhere.[15,16] Here we will just review the most important relations. In a SCF theory the observable segment densities are a functional of the so-called segment potentials (which are, by means of a mean-field construction, a type of external field that depends on the z-coordinate), and the segment potentials are a functional of the segment densities. Typically in the present system there are reflecting boundary conditions near $z=1$ and near $z=M$, and the interface between A/B is positioned roughly near $z=M/2$. The reflecting boundaries guarantee that all densities in $z=0$ equal those in $z=1$ and similarly the densities in $z=M+1$ equal those in $z=M$. Further the equations are solved using an incompressibility constraint. This last condition implies that on average each lattice layer is exactly filled or, mathematically,

$$\sum_i \varphi_i(z)=\sum_i \frac{N_i(z)}{L}=1, \tag{1}$$

where $N_i(z)$ is the number of units that molecules of type i have in layer z. Equation (1) also defines φ as the volume fraction of segments. The incompressibility constraint thus prevents that there are unoccupied sites. Note that the incompressible three-component system can also be interpreted as a two-component lattice-gas where the positions of one of the monomeric components are interpreted as vacant sites.

The SCF method thus naturally splits up into two separate parts which can be introduced briefly as follows.

D. From segment potentials to densities

In this section we assume that for each molecule type, $i,j=P_N,A,B$, or segment type $x,y=P,A,B$ there exists potential profiles $u_i(z,s)=\Sigma_{x=P,A,B}\delta^x_{i,s}u_x(z)$, where $u_x(z)$ is the potential felt by segments of type x in layer z, $u_i(z,s)$ is the potential felt by segment s of molecule i in layer z, and $\delta^x_{i,s}$ is the chain architecture operator, which assumes the value 1 when segment s of molecule i is of the type x and zero otherwise. Correspondingly, free segment weighting factors are defined as the Boltzmann weight, $G=\exp(-u/kT)$, where kT is the thermal energy, and the same labels and parameters carry over from the u to the G. These free segment weighting factors are used to compute the segment densities. The operations that need to be performed are conceptually simple; (i) one has to generate all possible and allowed conformations of the molecules in the system, (ii) determine the external potential felt by each of these conformations, (iii) use the Boltzmann weight to find a weighting factor for these conformations, and (iv) normalize them to obtain the probability of finding them in the system. For long chain molecules the number of conformations is too large to do this. The problem is solved by introducing Markov statistics. In this approach the chains are ghostlike and can visit previously occupied sites. The only requirement is that two consecutive segments along the chain are sitting on neighboring sites on the lattice. In this Markov approximation very efficient methods are available to obtain the segment densities from the potentials. To illustrate this, two complementary chain end distribution functions $G_i(z,s|1)$ and $G_i(z,s|N)$ are introduced. These two quantities collect the statistical weight of all chain conformations of complementary fragment of the chain, from the first segment to and including segment s and from the last segment N to and including segment s, respectively. The product of these two quantities is a measure for the probability to find segment s of molecule i at coordinate z,

$$\varphi_i(z,s)=C_i\frac{G_i(z,s|1)G_i(z,s|N)}{G_i(z,s)}, \tag{2}$$

where the denominator corrects for the fact that the potential field for segment s in coordinate z is accounted for in both complementary chain end distribution functions. C_i is a normalization which can be found easily and will be discussed below. There exists a propagator scheme which links the chain end distribution functions to those that correspond to chain fragments that are one segment shorter,

$$G_i(z,s|1)=G_i(z,s)\sum_{z'=z-1,z,z+1}\lambda_{z-z'}G_i(z',s-1|1),$$

$$G_i(z,s|N)=G_i(z,s)\sum_{z'=z-1,z,z+1}\lambda_{z-z'}G_i(z',s+1|N). \tag{3}$$

These equations are started by the condition that the chain end distribution function of a walk of one segment equals the corresponding free segment distribution function, $G_i(z,N|N)=G_i(z,N)$ and $G_i(z,1|1)=G_i(z,1)$.

Equations (2) and (3) reduce for monomeric components to the Boltzmann equation,

$$\varphi_x(z)=C_xG_x(z)\quad x\in\{A,B\}. \tag{4}$$

From Eqs. (2) to (4) it is straightforward to collect the segment densities per segment type. These will be used in the next step where the segment potentials are computed.

E. From segment densities to potentials

At this point we assume that the segment densities are available. The segment potentials are a function of these densities. Here we account for two terms,

$$u_x(z)=u'(z)+\sum_y \chi_{xy}\left(\sum_{z'=z-1,z,z+1}\lambda_{z-z'}\varphi_y(z')-\varphi_y^b\right). \tag{5}$$

Downloaded 28 Feb 2012 to 137.224.252.10. Redistribution subject to AIP license or copyright; see http://jcp.aip.org/about/rights_and_permissions

The first term is a Lagrange field coupled to the space-filling constraint. The second term in Eq. (5) accounts for short-range nearest-neighbor contacts parameterized by Flory–Huggins interaction parameters χ_{xy}. For given segment types x,y these parameters can be measured and are tabulated for many polymer systems. The potentials are normalized to be zero in the bulk and for this reason the bulk volume fraction of component y is subtracted in Eq. (5). Note that the segment potential is nonlocal due to the nearest-neighbor contact a segment x in layer z can have with segments of type y in $z'=z-1, z+1$. Long-range contributions to the segment potentials (e.g., van der Waals contributions) can in principle be included in Eq. (5) but in the standard SF SCF model this is not done.

F. The solution

The above set of equations is closed and can be solved. This is done routinely using a Newton-type iteraction scheme. Details about this procedure can be found elsewhere.[16] For two out of three components we fix the total amount of molecules in the system. The amount of A in equivalent monolayers is given by, $\theta_A=M/2$ (this forces the $A-B$ interface somewhere halfway the system) and the normalization of this component is

$$C_A=\frac{\Sigma_z\varphi_A(z)}{\Sigma_z G_A(z)}=\frac{\theta_A}{\Sigma_z G_A(z)}=\varphi_A^b. \tag{6}$$

The adsorption isotherm for the polymer chains is found by increasing in steps the amount of polymer in the system. The corresponding normalization is given by

$$C_P=\frac{\theta_P}{\Sigma_z G_P(z,N|1)}=\frac{\varphi_P^b}{N_P}. \tag{7}$$

The normalization of the solvent B follows from the condition that in the reference bulk phase the overall density should be unity,

$$C_B=1-\varphi_P^b-\varphi_A^b=\varphi_B^b. \tag{8}$$

In the limit of a homogeneous solution the SF SCF theory reduces to the Flory–Huggins theory.[18] For this reason it is possible to evaluate the bulk phase behavior of the system from this theory.

G. Adsorption isotherms

Each SCF solution gives a point for an adsorption isotherm. Moreover, for a given solution of the SCF equations one can evaluate the partition function and from this various thermodynamic and mechanical parameters of interest follow. Below we will discuss the excess adsorbed amount of the polymer component defined in the case that the polymer solubility characteristics are chosen to be symmetric with respect to the two bulk solvents. In this case the excess adsorbed amount of the polymer does not depend upon the choice of the dividing surface,

$$\theta_P^{\mathrm{exc}}=\sum_z \varphi_P(z)-\varphi_P^b=\theta_P-M\varphi_P^b. \tag{9}$$

For each component i the chemical potential μ_i is constant throughout the system. It is most conveniently expressed in terms of the composition of one of the bulk phases. For polymeric components the equation can be expressed as

$$\frac{\mu_i-\mu_i^*}{kT}=\ln\varphi_i^b+1-N_i\sum_j\frac{\varphi_j^b}{N_j}-\frac{N_i}{2}\times\sum_x\sum_y(\varphi_x^b-\delta_i^x)\chi_{xy}(\varphi_y^b-\delta_i^y), \tag{10}$$

where δ_i^x is unity when molecules of type i are composed of segments of type x and zero otherwise.

When there are steps in the adsorption isotherms the condition for the transition is found by an equal area procedure (Maxwell construction). Equivalently, and more conveniently, one can find such a transition point by plotting the interfacial tension as a function of the chemical potential. The crossing point in such a curve corresponds to the equilibrium point between the two adsorbed amounts. The interfacial tension follows from the partition function and can be written in the form,

$$\frac{\sigma b^2}{kT}=-\sum_z\left[\sum_i\frac{\varphi_i(z)-\varphi_i^b}{N_i}+\frac{u'(z)}{kT}+\frac{1}{2}\sum_x\sum_y\chi_{xy}\{\varphi_x(z)\langle\varphi_y(z)\rangle-\varphi_x^b\varphi_y^b\}\right]. \tag{11}$$

IV. PARAMETERS

As said above we will consider systems where there are two monomeric components that have effectively repulsive interactions such that there exists a solubility gap. This is the case for $\chi_{AB}>2$. The higher this value the larger the net repulsion is between the units and the stronger the liquids will segregate leaving a more and more sharp interface. A value of 2.2 will already yield an interface that is just a few molecules in width. The polymer chains have a fixed length of $N_P=100$. We will examine systems that are symmetric with respect to interchange of the two solvents A and B (and hence with respect to interchange of the A-rich phase and the B-rich phase). The solubility of the polymer in the solvents is bound to some upper limit. This is guaranteed when $\chi_{AP}=\chi_{BP}>\frac{1}{2}(1+N_P^{-0.5})^2=0.605$. The indicated lower limit represents the critical value at which the polymer becomes completely miscible with a monomeric solvent. This value is also a reasonable indication for the limit where the polymer becomes miscible with the binary solvent mixture discussed in the present paper. The lattice used consisted typically of $M=100$ layers, but to avoid boundary effects this value was increased for relative low values of χ_{AB}. The step probabilities were fixed to $\lambda_1=\lambda_{-1}=\lambda_0=1/3$. This choice is popular as relative to a cubic lattice there are only small adverse effects of the discretisation of space. SCF solutions were generated with a precision of 7 significant digits.

V. RESULTS

Wetting problems are, because there are at least three phases involved, complex. It is therefore of significant help to have insight in the bulk phase behavior of the systems

Downloaded 28 Feb 2012 to 137.224.252.10. Redistribution subject to AIP license or copyright; see http://jcp.aip.org/about/rights_and_permissions

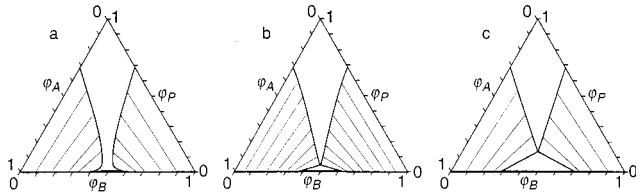

FIG. 1. Ternary phase diagrams for systems containing the components P_{100}, A_1, and B_1 as calculated by the Flory–Huggins theory. Parameters $\chi_{PA}=\chi_{PB}=1.02$, and the solvent demixing parameter was (a) $\chi_{AB}=2.02$, (b) $\chi_{AB}=2.05$, (c) $\chi_{AB}=2.125$. The diagrams show how the three-phase region (panel b and c) vanishes upon the approach of the χ_{AB} towards the critical value of 2. In panel 1 there are 3 two-phase regions.

studied. The SF SCF theory reduces for bulk systems to the well-known Flory–Huggins theory for which it is relatively straightforward to generate ternary phase diagrams. In Fig. 1 we show a few typical ones which are in the parameter range studied below. The three examples differ in the value of the solvent demixing parameter χ_{AB} and all have the same polymer–solvent interaction of $\chi_{PA}=\chi_{PB}=1.02$. The ternary phase diagrams show a three-phase coexistence region [Figs. 1(b), 1(c) inner triangles] and three two-phase regions connected to them (a few tie lines connecting coexisting phases are given). Of interest is the way the three-phase triangles change upon a decrease of χ_{AB}. As the $A-B$ critical point depends on the polymer–solvent interactions and the polymer–solvent critical point depends on the interaction between the solvents, the outcome is not trivial. The three-phase solubility gap as shown in Figs. 1(b), and 1(c) by the inner triangles shrinks upon decrease of χ_{AB}. In Fig. 1(a), the three-phase solubility gap is lost and three two-phase regions remain. When $\chi_{AB}<2$ only two two-phase regions are left. The systems that we are interested in are balanced with respect to the amount of A and B in the system; they thus are on a vertical line from the top of the phase triangles. Our interest will also be limited to those systems that have three-phase coexistence [e.g., Figs. 1(b) and 1(c)]. From the series shown in Fig. 1 we finally draw the conclusion that for values of χ_{AB} close to 2, there is no three-phase coexistence. In this region the polymer rich phase dissolves completely into the solvent phases; wetting ceases to exist here.

Wetting of a polymer phase at a simple L/L interface has recently been studied by Van Eijk and Leermakers.[13] In this work the width of the interface was kept constant (χ_{AB} was fixed) and attention was given to the variables associated with the polymer. Here we will extend this work and look also to the interfacial width as a control variable.

In Fig. 2(a) a few adsorption isotherms are presented where we have varied the polymer solubility parameter at constant interfacial width ($\chi_{AB}=2.15$). From this figure it is seen that a first-order wetting transition can be induced by using the polymer–solvent interaction as a control variable. There is a curve that corresponds to the case that the polymer adsorption at the interface occurs without any special features $\chi_{PA}=\chi_{PB}=1.0$. There is an adsorption isotherm typical for partial wetting $\chi_{PA}=1.03$. The curve that (almost) corresponds to the wetting transition point happens to be at $\chi_{PA}=1.02$ and the curve for $\chi_{PA}=1.01$ is a typical example of an adsorption isotherm with a prewetting step. The $\chi_{PA}=1.01$ condition is close to the prewetting critical point. The van der Waals loop is still present but rather small. In Fig. 2(b) the corresponding surface-tension vs chemical-potential curves are plotted. Note that all the lines in this graph end at $\Delta\mu_P=\mu_P-\mu_P^{\#}=0$, where $\mu_P^{\#}$ is the chemical potential at the saturation value of polymer in the solvents. This is natural as thick polymer layers in between the $A-B$ interface can only exist at coexistence. The surface tension typically decreases with increasing chemical potential. This is so for all point for the $\chi_{PA}=1.0$ case. The cusp seen for $\chi_{PA}=1.01$ [see inset in Fig. 2(c)] is in line with the stepwise increase in adsorbed amount. The crossing point of the lines corresponds with the transition condition. The lower lines are the stable lines. The $\sigma(\Delta\mu_P)$ exhibits a discontinuity in the first derivative at the step. For $\chi_{PA}=1.02$ the crossing of the lines coincide with the $\Delta\mu_P=0$ axis. From this it is concluded that the wetting transition is indeed at $\chi_{PA}=1.02$. The partial wetting case shows an unfinished cusplike figure; there is no crossing of lines.

As told above there are two interaction parameters in the system. In Fig. 3 we examine the second one. For a fixed value of the polymer–solvent interaction set of adsorption isotherms are shown which differ with respect to the AB interaction. One of the reasons for the polymers to adsorb onto the AB interface is to screen unfavorable AB contact. At constant polymer–solvent interaction it is thus natural that a higher affinity isotherm is found for higher values of χ_{AB}. In Fig. 3(a) three adsorption isotherms and in Fig. 3(b) the corresponding surface-tension-vs-the-chemical-potential plots are presented. Inspection of these curves shows that there must be two consecutive wetting transitions, or equivalently that there is a window of partial wetting. Both at strong

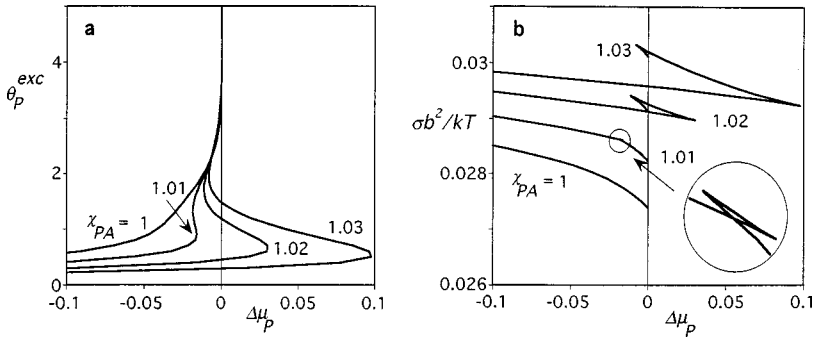

FIG. 2. (a) Adsorption isotherms (excess adsorbed amount vs the chemical potential) of the polymer component in the $A-B$ interface. (b) Dimensionless surface tension vs the chemical potential of the polymer component. Values for the polymer–solvent interaction parameters are indicated and the $\chi_{AB}=2.15$. In (b) the inset gives an expanded view of the cusps for the case $\chi_{PA}=1.01$. The position of the step in the isotherm of (a) coinsides with the point where the lines cross in (b) This is equivalent to using a Maxwell construction.

Downloaded 28 Feb 2012 to 137.224.252.10. Redistribution subject to AIP license or copyright; see http://jcp.aip.org/about/rights_and_permissions

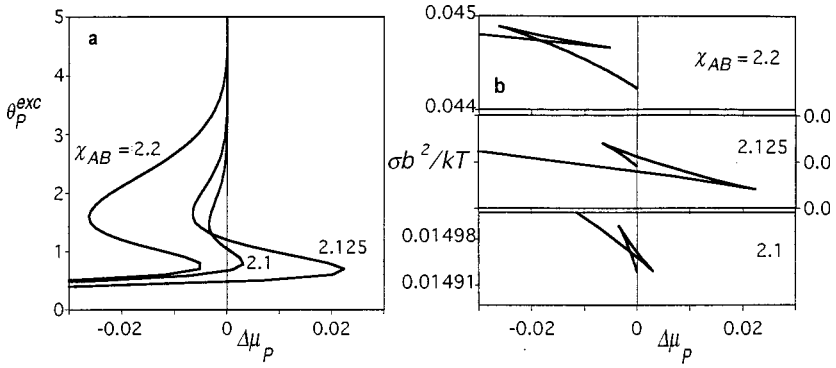

FIG. 3. (a) Adsorption amounts (adsorption isotherms) and (b) normalized surface tension against the chemical potential of the polymer component at a fixed polymer–solvent interaction parameter $\chi_{PA}=\chi_{PB}=1.02$ for three values for the effective repulsion between A and B units as indicated. The position of the step in the isotherms in (a) can be obtained from a Maxwell construction or equivalently this can be deduced from the crossing points in (b).

segregation $\chi_{AB}>2.15$ and weak segregation $\chi_{AB}<2.11$ of the two liquids we find isotherms that correspond to complete wetting. Both at weak and at strong segregation we find a step in the adsorption isotherms which indicates that both transitions are first order. From the cusps in Fig. 3(b) it is concluded that only the $\chi_{AB}=2.125$ case corresponds to partial wetting and that there must be a wetting transition both above and below this value.

The wetting scenario as shown in Fig. 3 is expected to be subject to change upon variations of the polymer–solvent interaction parameter. In Fig. 4 a selection of adsorption isotherms is presented which belong to systems with a slightly better polymer–solvent interaction of $\chi_{PB}=\chi_{PA}=1.011$. This value was chosen as in this case all isotherms correspond to complete wetting; all isotherms, in fact for all relevant values of χ_{AB} also those that are not shown in Fig. 4, diverge upon the approach of the saturation value. Quite unexpectedly, and this is a major result of this paper, there are still steps in the adsorption isotherm which resemble the prewetting steps discussed above. These steps occur in a well-defined range, $2.11<\chi_{AB}<2.18$. $\chi_{AB}=2.11$ can be called the lower critical χ_{AB} and $\chi_{AB}=2.18$ the upper critical χ_{AB} for these steps in the isotherms. The physical interpretation of the step in the adsorption isotherm is that a microscopically thick polymer film and a mesoscopically thick one can coexist.

A standard procedure for this type of phase transition is to connect the compositions of the layers that can coexist to form so-called binodals (see, e.g., Ref. 3). In this case a closed-loop phase diagram emerges. Closed loops are not uncommon in (multicomponent) bulk phase diagrams, but they are to our information not reported for interfacial phase equilibria. In Fig. 4 a closed-loop phase diagram is plotted by the dashed line (which was constructed from a much larger set of adsorption isotherms). At these critical points the adsorption isotherms go over from having an inflection point (second-order transition) to isotherms which feature van der Waals loops. The very first van der Waals loops have rather tiny unstable regions and therefore the critical points are usually rather difficult to examine with high precision. Away from the critical points the van der Waals loops are much more pronounced and can be analyzed routinely.

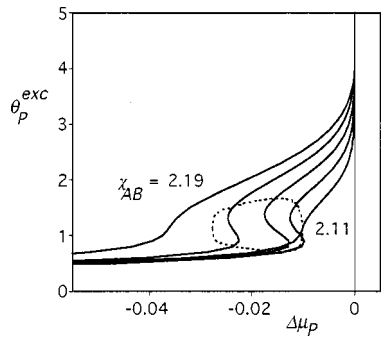

FIG. 4. Excess adsorbed amount of the polymer component in the AB interface as a function of the (normalized) chemical potential. The polymer–solvent interaction was fixed to $\chi_{PB}=\chi_{PA}=1.011$, and the χ_{AB} was varied in steps of 0.02 from 2.11 until 2.19 (the extremes are indicated in the plot). The dashed line is the closed-loop phase diagram which is found by connecting the transition adsorbed amounts with each other.

The single difference between the systems presented in Figs. 3 and 4 is the difference in solubility of the polymer in the solvent(s). When the solubility is low, there is a window of partial wetting, bracketed both at weak and at strong segregation by first-order wetting transitions. When the solubility is a bit higher the first-order transitions vanish. Apparently the window for partial wetting closes upon increasing the solubility of the polymer for the solvent. The steps in the isotherms in Fig. 4 are the remainder of the prewetting steps, but remarkably there is no longer a corresponding wetting transition as at fixed $\chi_{PB}=\chi_{PA}=1.011$ there is complete wetting for all χ_{AB}.

It is instructive to examine the fate of the prewetting line $\Delta\mu_P(\chi_{AB})$ when the system changes from having two wetting transitions to none by changing χ_{PA}. The whereabouts of prewetting lines can be analyzed in wetting phase diagrams. In Fig. 5 such a wetting phase diagram is presented for the present system. On the x-axis the χ_{AB} value, and on the y-axis the normalized chemical potential is plotted. Lines in this phase diagram are lines of first-order phase transitions. One of these is the $\Delta\mu_P=0$ line. Below this line there is just a two-phase system (A-rich, B-rich) and above this line there are three phases (A-rich, B-rich and a polymer-rich phase). The prewetting steps in the adsorption isotherms are first-order transitions. For values of the polymer–solvent interaction parameter $\chi_{PA}>1.018$ there are two wetting transitions and connected to both wetting transitions there are prewetting lines extending into the $\Delta\mu_P<0$ half-space. However, at about $\chi_{PA}=1.018$ the two wetting transitions merge and obviously also the prewetting lines merge. For $\chi_{PA}<1.018$ the prewetting lines are disconnect from the co-

Downloaded 28 Feb 2012 to 137.224.252.10. Redistribution subject to AIP license or copyright; see http://jcp.aip.org/about/rights_and_permissions

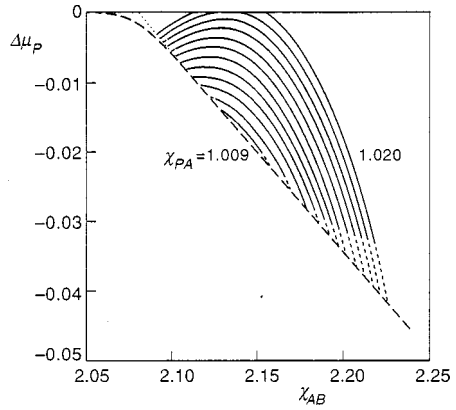

FIG. 5. Wetting phase diagram. The chemical potential of the wetting component P_N against the control parameter χ_{AB} for various values of the polymer–solvent interaction parameter in the range $\chi_{PB}=\chi_{PA}=1.009$ to 1.020 (with steps of 0.001). The solid part of the lines are computed. The short dashed extensions towards the prewetting critical point are drawn by hand based also on information from Figs. 6 and 7. The prewetting critical points are connected by a dashed line. The way this line approaches $\Delta\mu_p=0$ is sketched on the basis of data presented in Fig. 11.

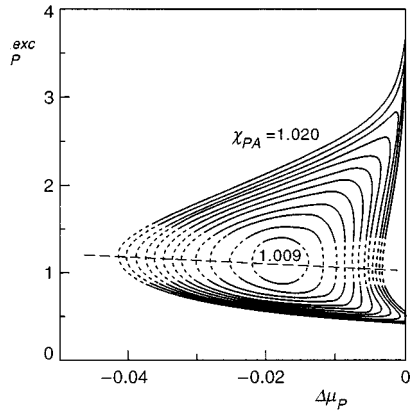

FIG. 6. Interfacial phase diagrams. The amount of polymer at the liquid interface in both the microscopically thin films (lower parts of the loops) and the mesoscopically thin layers (upper parts of the loops) which coexist at the points of the prewetting steps as a function of the chemical potential. The parts of the phase diagrams near the critical points are not computed but estimated also on the basis of data presented in Figs. 5 and 7. The polymer–solvent interaction parameters are indicated and are the same as in Figs. 5 and 7. The upper and lower critical points are connected to each other by a dashed line for illustrative purposes.

existence line $\Delta\mu_P=0$. Now we understand that the prewetting lines are still there in absence of the wetting transition(s). The length of the detached prewetting lines reduces subsequently with decreasing χ_{PA}. The prewetting line shrinks to one point near $\chi_{PA}=1.009$. For $\chi_{PA}<1.009$ there is no step in the isotherm any longer and the polymer wets the interface without any special features when the χ_{AB} interaction parameter is used as control variable.

It is of special interest to note that the upper and lower prewetting critical points, which are points of second-order phase transitions, all fall on a curve which is remarkably linear over a wide range of parameters. We will return to this point below.

It is possible to assemble as was done in Fig. 4, phase diagrams in coordinates which give some information on the structure (excess adsorbed amounts) of the microscopically and mesoscopically thin films that coexist. In Fig. 6 a set of those phase diagrams is shown. For the range of $1.009<\chi_{PA}<1.018$ the phase diagrams are of the closed-loop type. For values $\chi_{PA}>1.018$ the phase diagrams are not closed; the excess adsorbed amount of the mesoscopically thick branch of the phase diagram diverges (becomes macroscopically thick) upon the approach of the bulk coexistence line $\Delta\mu_P=0$. Near $\chi_{PA}=1.009$ the closed loops shrink to a point and subsequently vanish.

One more way to present the data is to plot the excess adsorbed amount of both the microscopically and the mesoscopically thick film that coexists as a function of the χ_{AB} value where the prewetting transition takes place (Fig. 7). This is perhaps the most common way to present the phase diagram of the system, as χ_{AB} can be seen as the inverse temperature and the excess adsorbed amounts as a measure for the composition of these phases. Obviously, in the range $1.009<\chi_{PA}<1.018$ the phase diagrams are closed. The loop shrinks to a point and vanishes near $\chi_{PA}=1.009$. The phase diagrams open up as soon as wetting transitions emerge in the system near $\chi_{PA}=1.018$.

As told above, the phase diagrams are not very accurate near critical points. However combining the data of Figs. 5–7 gives a good impression how the various missing parts of the calculations should go. We have extrapolated these parts (by hand) and filled them in by dashed line—parts in Figs. 5–7.

VI. DISCUSSION

Both at very strong *AB* segregation and at weak *AB* segregation the polymer wets the *AB* interface. If there is a region of partial wetting in this system, it is bracketed by two wetting transitions in such way that the previous statement remains true. It is easily understood why the polymer wets the interface at strong segregation. In this case the surface tension of the *AB* interface is high and the polymer spreads

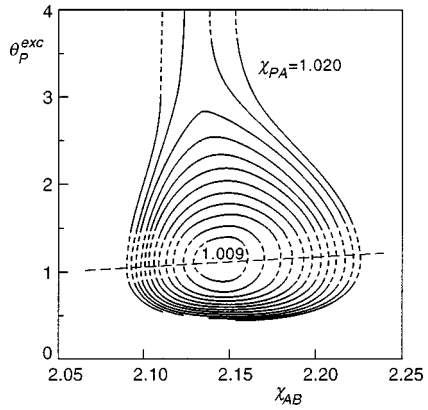

FIG. 7. Interfacial phase diagrams. The amount of polymer at the liquid interface in both the microscopically thin films (lower parts of the curves) and the mesoscopically thin films (upper parts of the curves) that coexist at the prewetting step as a function of the effective *AB* repulsion χ_{AB} in the system. The dashed lines near the critical points are drawn by hand also using information from Figs. 5 and 6. The upper and lower critical points are connected by a dashed line for illustrative purposes.

Downloaded 28 Feb 2012 to 137.224.252.10. Redistribution subject to AIP license or copyright; see http://jcp.aip.org/about/rights_and_permissions

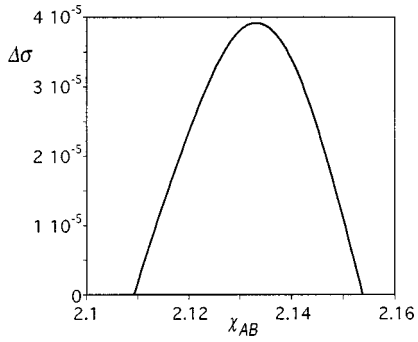

FIG. 8. Difference between the surface tension of the $PA+PB$ interfaces and the surface tension of the AB interface $\Delta\sigma=2\sigma_{PA}-\sigma_{AB}$ at the three-phase coexistence condition in the partial wetting condition for $\chi_{PA}=\chi_{PB}=1.02$.

along the interface to remove the AB contacts. The wetting transition at weak segregation is expected from the Cahn-type argument mentioned in the introductory wetting theory section. In the first instance one would expect that upon reducing the value of the χ_{AB} the AB interface becomes critical. However, the $P-A$ and thus $P-B$ miscibility increase also when χ_{AB} is reduced. We can define an effective polymer solvent interaction as were the polymer just in a single solvent,

$$\chi_{PS}^{\text{eff}}=\varphi_A\chi_{PA}+\varphi_B\chi_{PB}-\varphi_A\chi_{AB}\varphi_B. \tag{12}$$

The polymer concentration in the solvent rich phases is typically very low and thus we may use $\varphi_A+\varphi_B=1$ and Eq. (12) reduces to

$$\chi_{PS}^{\text{eff}}=\chi_{PA}-\chi_{AB}\varphi_A+\chi_{AB}\varphi_A^2, \tag{13}$$

where we used $\chi_{PA}=\chi_{PB}$. Not too far from the AB-critical point we can estimate the density of solvent A in the B-rich phase from the Van der Waals theory (see, e.g., Ref. 19),

$$\varphi_A=\frac{1}{2}-\sqrt{\frac{3}{8}(\chi_{AB}-2)}\approx\frac{1}{2}-\left(1-\frac{1}{\chi_{AB}}\right)\sqrt{\frac{3}{8}\chi_{AB}}. \tag{14}$$

Obviously, this concentration increases with decreasing χ_{AB}. The combination of Eq. (14) with Eq. (13) shows that the χ_{PS}^{eff} reduces more than linearly with χ_{AB}. It is likely that the system can evolve to $\chi_{PS}^{\text{eff}}<0.605$ where the polymer becomes miscible with the solvents. This analysis is confirmed by comparison of the surface tensions of the PA and PB interfaces with that of the AB interface. A typical result is presented in Fig. 8, where the difference between the relevant surface tensions, $\Delta\sigma=2\sigma_{PA}-\sigma_{AB}$, is plotted in the range of partial wetting, $\sigma_{AB}<\sigma_{PA}+\sigma_{PB}=2\sigma_{PA}$. The wetting transition occurs when $\Delta\sigma=0$. The wetting transition on the weak segregation side of the A-B phases is thus because $2\sigma_{PA}$ drops more quickly with χ_{AB} than σ_{AB}. Indeed upon reduction of χ_{AB} at fixed $\chi_{PA}=\chi_{PB}$ the system moves more slowly towards its AB critical point than towards the two critical points for the PA and PB phases. As the three possible critical points are not approached simultaneously, i.e., we do not hit the tricritical point in the system, the result is compatible with the Cahn argument; the polymer rich phase tends to become critical both with the A and B phase, and thus the interfacial tension $\sigma_{PA}=\sigma_{PB}$, and the difference $\Delta\sigma=2\sigma_{PA}-\sigma_{AB}$ approach zero in different ways such that before the AP and BP interfaces become critical there is a wetting transition in the system. The absolute values of the surface tensions however are not yet extremely small. In Fig. 8 they increase approximately linearly with χ_{AB} in the regime shown, $\sigma_{AB}(\chi_{AB}=2.11)\approx0.0177$ and $\sigma_{AB}(\chi_{AB}=2.154)\approx0.03$.

In a considerably asymmetric case, where the polymer prefers one phase over the other, the scenario is likely to be fundamentally different. In this case the transitions near the critical condition for the AB system involve the uptake of the polymer phase into the solvent that has the highest affinity for the polymer. This last case can be considered as a wetting transition for the high affinity solvent on the polymer phase (or the drying transition for the low affinity solvent). Again this system is not considered here. Asymmetric cases are left for future work.

Figures 5–7 give a detailed survey of the wetting characteristics of this system. There are a few interesting issues to elaborate on. Inspection of Figs. 6 and 7 shows that the prewetting critical points fall on an almost horizontal line, characterized by an excess amount in the range $1<\theta_P^{\text{exc}}<1.2$. This does not mean that the prewetting polymer film is just one (lattice) layer thick. In Fig. 9(a) typical density profiles are collected which correspond to a system reasonably close to the upper prewetting critical point (solid lines), and in Fig. 9(b) the corresponding density profiles are given for the lower critical points. The χ_{PA} was fixed to a value for which the closed loop has its maximum size $\chi_{PB}=\chi_{PA}=1.018$. Although the excess amount is the same in both cases, the structure of the interface depends strongly on the magnitude of the repulsion between the solvents. The density of the polymer phase increases, and then the thickness of the

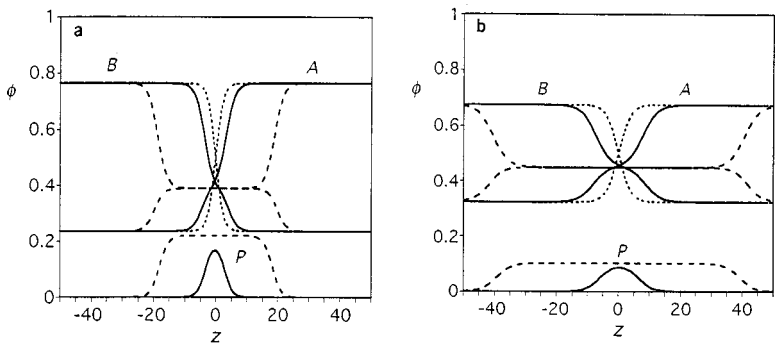

FIG. 9. Some density profiles through a cross-section of the interface at (a) the upper critical value $\chi_{AB}=2.225$, (b) the lower critical value $\chi_{AB}=2.09$. The following profiles are shown: (i) the bare $A-B$ interface $\theta_P=0$ (dotted lines); (ii) near the critical conditions $\theta_P^{\text{exc}}=1.2$ (solid lines); (iii) at coexistence $\theta_P=8$ (dashed lines). The polymer–solvent interaction is given by $\chi_{PB}=\chi_{PA}=1.018$. The lattice layers are arbitrarily numbered.

Downloaded 28 Feb 2012 to 137.224.252.10. Redistribution subject to AIP license or copyright; see http://jcp.aip.org/about/rights_and_permissions

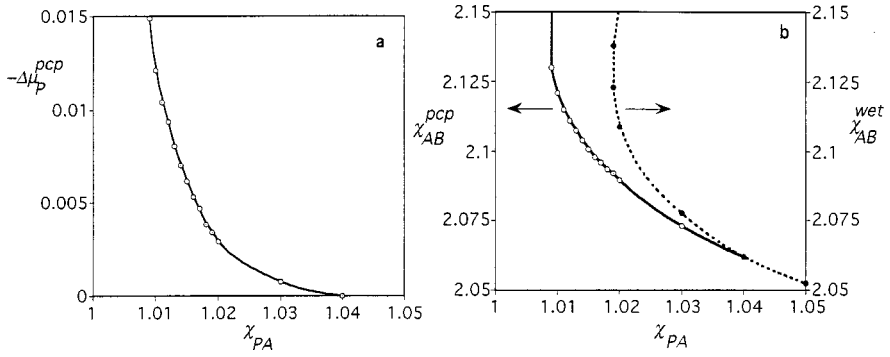

FIG. 10. (a) The normalized chemical potential at the prewetting critical point as a function of the polymer–solvent interaction parameter χ_{PA}. (b) The χ_{AB} at the prewetting critical point (open symbols) and χ_{AB} at the wetting transition (closed symbols; dotted line) as a function of the polymer–solvent interaction parameter. The points are extracted from Figs. 5 and 11. The two lines meet in the multicritical point.

polymer film decreases upon an increase of the χ_{AB}. The polymer film assumes its maximum density of $\phi_P<0.2$ near $z=0$ and the film thickness is more than $10b$ (lattice layers). Thus the polymer layer is considerably swollen by the two solvents, most significantly for the case with $\chi_{AB}=2.225$. The radius of gyration of the polymer component is approximately $4b$, and thus the polymer molecules are not strongly deformed. The polymer density does not reach a plateau (bulk) value and thus we should consider all polymers to be interfacial molecules. For comparison the density profiles of the bare $A-B$ interfaces are given in Figs. 9(a) and 9(b) (dotted lines). With decreasing χ_{AB} the intrinsic AB interfacial width increases. Clearly the width of the interfaces broadens when there are polymers in the system. Also for comparison we give in Figs. 9(a) and 9(b) (dashed lines) the profiles for the case that there is a wetting film in between the $A-B$ interface. From these graphs one can see the width of the $A-P$ and $B-P$ interfaces. As noted above as well, upon decreasing the χ_{AB}, the system also moves considerably closer to the $A-P$ and $B-P$ critical points. This explains why the $A-P$ and $B-P$ interfaces broaden upon a decrease of χ_{AB}. This confirms the conclusion of Fig. 8 that upon decreasing χ_{AB} the system moves more dominantly to the critical points of $A-P$ and $B-P$ rather than $A-B$. Returning now to the profiles seen for the prewetting critical conditions, we conclude that the interfacial profiles are a combination of the $A-P$ and $B-P$ interfaces more than the bare $A-B$ interface.

Another point of interest, already mentioned above, is that the critical points of the prewetting lines form a curve which is in the parameter space selected in Fig. 5 linear over a wide region. At present it is not clear why all these points fall on such a straight line. It is tempting, but as we will see wrong, to extrapolates this line to the $\Delta\mu_P=0$ axis (Fig. 5, the dotted extrapolation).

In Fig. 10(a) the line of second-order phase transitions is presented as the chemical potential at the prewetting critical point versus the polymer solvent parameter χ_{PA}; $\Delta\mu_P^{pcp}(\chi_{PA})$ (where pcp refers to the prewetting critical point). Again the interesting point of this graph is the value of χ_{PA}, where the $\Delta\mu_P^{pcp}=0$. By the nature of the curve it is not easy to extract an accurate value of χ_{PA}, where $\Delta\mu_P^{pcp}=0$, however, it is clear that at $\chi_{PA}=1.04$ the prewetting lines are within numerical accuracy. In Fig. 10(b) the corresponding view graph of the χ_{AB} at the prewetting critical point is given, also as a function of the polymer-solvent interaction χ_{PA}. Besides the data extracted from Fig. 5, information on the wetting behavior at $\chi_{PA}=1.03$, 1.04, and 1.05 included as well. Relevant adsorption isotherms for the condition that $\chi_{PA}=1.03$,1.04 are given in Figs. 11(a) and 11(b). The adsorption isotherms of Fig. 11(b) show that in this case there is a second-order wetting transition in the system, whereas in the conditions of Fig. 11(a) the transition is still first order. We thus conclude that there is a multicritical point in the system which is located near $\chi_{AB}=2.062$, and χ_{PA} of near 1.04.

The conclusion must be that the extrapolation of the line of second-order prewetting critical points as suggested above is not allowed and that this line bends over and connects to the $\Delta\mu_P^{cep}=0$ with a much smaller angle (possibly with angle zero). The actual crossing point of the line of second-order prewetting critical points touch the $\Delta\mu_P^{cep}=0$ line has a physical meaning. For values of χ_{AB} smaller than this con-

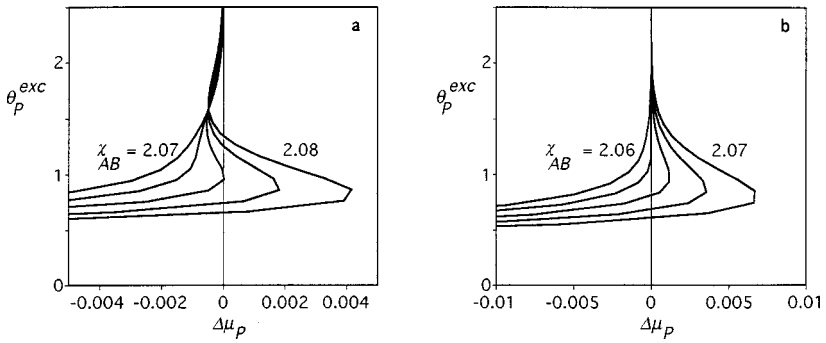

FIG. 11. Adsorption isotherms for a fixed polymer–solvent interaction parameter of (a) $\chi_{PA}=1.03$ and (b) $\chi_{PA}=1.04$. The value of the χ_{AB} parameter was varied with steps of 0.0025 in the indicated range.

Downloaded 28 Feb 2012 to 137.224.252.10. Redistribution subject to AIP license or copyright; see http://jcp.aip.org/about/rights_and_permissions

nection point the wetting transitions are second order. For the values above this connection point the wetting transitions are first order.

In Fig. 10(b) we have also plotted the χ_{AB} at the wetting transition (dotted line closed symbols). The point where $\chi_{AB}^{\mathrm{wet}}=\chi_{AB}^{\mathrm{pcp}}$ corresponds to the multicritical point χ_{AB}^{mcp}. Thus for $\chi_{AB}^{\mathrm{wet}}<\chi_{AB}^{\mathrm{pcp}}$ are wetting transitions of the second-order type. In other cases the wetting transition is first order.

A polymer-rich phase at a liquid–liquid interface is still a very simple system. An interesting analogy of the present problem may be noticed with the wetting of the middle phase in a balanced Winsor III microemulsion system. Recently there have been both experimental[10,11] and theoretical investigations[12] of this system. The surfactant rich middle phase is in between the oil and water phases. This middle phase can either wet the oil–water interface partially or completely. Wetting transitions can be generated by changing the temperature. The middle phase can be characterized by a length scale (correlation length) which corresponds to the typical distance between surfactant layers. This length scale is much larger than the size of the oil or water molecules. In our system the length scale connected to the polymers is also much larger than the size of the *A* or *B* monomers and therefore the physics is likely related. In the microemulsion system the middle phase only exists when the spontaneous curvature of the oil–water–surfactant system approaches zero. Therefore, this system may be near or at (balanced) the ''symmetrical'' conditions chosen in the present system.

It is of special interest that in this context it has been suggested that there are detached prewetting lines.[20] In the Winsor III system two wetting transitions may be expected upon a change in temperature. These transitions do not occur because the oil–water system becomes critical, but because the system can move either to a critical point of mixing of the microemulsion–water or the microemulsion–oil phases. These wetting transition differ from the ones discussed above and should be linked to the wetting scenarios mentioned above for the case that our system becomes asymmetric as to the role of *A* and *B*. It may be of interest to investigate whether the Ginzburg–Landau theory for these microemulsion systems can be used to model the present system as well. When doing so, it becomes possible to link the phenomenological parameters in a Ginzburg–Landau theory to the molecular parameters of the SF SCF theory.

In model studies of polymer blends it is customary to try to build a system with as much symmetry as possible. The molecular weight of the homopolymer melts is matched and the block-copolymer compatibilizer is composed of two blocks which each resemble one of the homopolymers in the system. In the same spirit we can imagine that one can set up systems with the characteristics discussed in the present paper. A suggestion is to take two (oligomeric) nonmiscible solvents and an alternating copolymer with repeat units similar to the solvents. This polymer may then be limited, but equally soluble, in both solvents. This type of system could be used to study the wetting behavior as discussed above.

As it is likely that some residual asymmetry with respect to interchange of the two solvents can never be removed from a system it remains essential to know how important asymmetrical interactions, i.e., when the polymer prefers one solvent phase over the other, are. There are additional and interesting effects of an asymmetry in the interactions. For example one should expect that the interface has a nonzero preferential curvature (cf., the effect on nonzero preferential curvature in microemulsions). Also it remains of interest to investigate the effect of the molecular weight of the polymer and the molecular weight disparity between solvents and polymer on the wetting behavior, in particular concerning the range of second-order transitions and the existence of detached prewetting lines. Some of these effects have already been examined before,[13] but the full picture is far from complete. We are planning to keep working on these issues in the near future.

VII. SUMMARY AND CONCLUSIONS

Wetting at liquid–liquid interfaces has been studied by means of a lattice-based self-consistent-field theory. In this theory it is possible to mimic molecular properties of the system. It features explicitly the relative size and chainlike character of the molecules, and the various interactions in the system. For this reason we might refer to this approach to be explicitly molecular based, in contrast to e.g., Ginzburg–Landau approaches to wetting which are basically phenomenological.

This study was restricted in several ways. The sizes of the three molecular components were fixed. Two monomeric bulk solvents *A*,*B*, and one polymer component with 100 repeat units were used. The system was always symmetric with respect to interchanging the solvents *A* and *B*. Thus the preferential curvature in the system remains zero throughout. There were only two interaction parameters in the system, namely the parameter accounting for the repulsion between the two monomeric solvents and the polymer-solvent interaction. The effect of these two parameters, in the domain of incomplete miscibility, was exhaustively studied. We have assumed that these parameters can be varied independently from each other.

At three-phase coexistence the $A-B$ interface is polymer wet when the polymer solvent interaction is good enough. When this is not the case it is possible to induce wetting transitions in this system by varying the width of the $A-B$ interface. In the case of partial wetting, i.e., when the polymer-rich phase sits as a lens in the $A-B$ interface, one can induce wetting by either increasing or decreasing the *AB* contact energy (at fixed polymer–solvent interactions). The wetting transition which occurs on the strong segregation side was found to be first order. The wetting transition on the weak segregation side, can either be first or second order. Wetting transitions below χ_{AB}^{mcp} are second order.

In a small region of polymer–solvent interaction parameters (in this case $1.009<\chi_{PA}<1.018$) detached prewetting lines are found. These prewetting lines are the remainders of the merging of the two first-order wetting transitions. The detached prewetting lines have been analyzed in detail. It was found that the prewetting critical points all fall on one straight line in the wetting phase diagram with coordinates (χ_{AB} and $\Delta\mu_P$). Only near $\Delta\mu_P=0$ the linearity is lost and

Downloaded 28 Feb 2012 to 137.224.252.10. Redistribution subject to AIP license or copyright; see http://jcp.aip.org/about/rights_and_permissions

the curve of second-order transitions bends over to connect to $\Delta\mu_P=0$ smoothly. Closed-loop phase diagrams were constructed for the behavior of the polymer film at the $A-B$ interface. The upper and lower critical points were all shown to have about the same excess amount of polymer (per unit area) in the interface. The critical thickness of a polymer film with this critical excess amount depends however strongly on the intrinsic width of the $A-B$ interface.

ACKNOWLEDGMENTS

This work is performed as a part of the program Computational Material Science (CMS) of the Dutch National Science Foundation (NWO) and financial support of GEP, Bergen op Zoom, is highly appreciated. The research of NAMB has been made possible by a fellowship of the Royal Netherlands Academy of Arts and Sciences. The authors want to thank Dr. P. Linse for making available the program for calculating the ternary phase diagrams and for the help in using it.

[1] M. Schick, in *Liquids at Interfaces*, Les Houches Session 48 NATO ASI, edited by J. Charvolin, J. F. Joanny, and J. Zinn-Justin (Elsevier, Amsterdam, 1990).
[2] P.-G. de Gennes, Rev. Mod. Phys. **57**, 827 (1985).
[3] H. T. Davis, *Statistical Mechanics of Phases, Interfaces, and Thin Films* (VCH, New York, 1996).
[4] J. D. van der Waals, Ph.D. thesis, State University of Leiden, The Netherlands, 1873.
[5] T. Young, Philos. Trans. R. Soc. London **95**, 65 (1805).
[6] P. S. de Laplace, Mécanique Céleste, suppl. au X. livre (1805).
[7] J. W. Cahn, J. Chem. Phys. **66**, 3667 (1977).
[8] K. Ragil, J. Meurnier, D. Broseta, J. O. Indekeu, and D. Bonn, Phys. Rev. Lett. **77**, 1532 (1996).
[9] J. O. Indekeu, K. Ragil, D. Bonn, D. Broseta, and J. Meunier, J. Stat. Phys. (to be published).
[10] Y. Seeto, J. E. Puig, L. E. Scriver, and H. T. Davis, J. Colloid Interface Sci. **96**, 360 (1983).
[11] M. Aratona and M. Kahlweit, J. Chem. Phys. **95**, 8578 (1991).
[12] G. Gompper and M. Schick, *Self-Assembling Amphiphilic Systems*, edited by C. Domb Lebowitz (Academic, London, 1994), Vol. 16.
[13] M. C. P. Van Eijk and F. A. M. Leermakers, J. Chem. Phys. **110**, 6491 (1999).
[14] J.-S. Wang and K. Binder, J. Chem. Phys. **94**, 8537 (1990).
[15] G. J. Fleer, J. M. H. M. Scheutjens, M. A. Cohen Stuart, T. Cosgrove, and B. Vincent, *Polymers at Interfaces* (Chapman and Hall, London, 1993).
[16] O. A. Evers, J. M. H. M. Scheutjens, and G. J. Fleer, Macromolecules **23**, 5221 (1990).
[17] L. J. M. Schlangen, F. A. M. Leermakers, and L. K. Koopal, J. Chem. Soc., Faraday Trans. **92**, 579 (1996).
[18] P. J. Flory, *Principles of Polymer Chemistry* (Cornell University Press, Ithaca, 1953).
[19] S. A. Safran, *Statistical Thermodynamics of Surfaces, Interfaces, and Membranes* (Addison–Wesley, Reading, 1994).
[20] M. Schick, Ber. Bunsenges. Phys. Chem. **100**, 272 (1996).

Downloaded 28 Feb 2012 to 137.224.252.10. Redistribution subject to AIP license or copyright; see http://jcp.aip.org/about/rights_and_permissions